HYPERSOUND FROM ELECTRO-STRICTIVE BEATING OF LONGITUDINAL LASER MODES

NORVAL LEON WARDLE

HYPERSOUND FROM ELECTROSTRICTIVE

BEATING OF LONGITUDINAL LASER MODES

by

Norval Leon Wardle
Lieutenant, United States Navy
B.S., Iowa State University, 1960

Submitted in partial fulfillment of the
requirements for the degree of

DOCTOR OF PHILOSOPHY

from the

NAVAL POSTGRADUATE SCHOOL
June 1968

ABSTRACT

A new method for generating pulses of hypersound by electrostrictive beating of two coherent light beams has been demonstrated. Three new procedures for generating the two required beams with a precise and predictable difference between their frequencies have been experimentally investigated. In the most practical of these a giant pulse ruby laser was forced to emit light at two frequencies. Techniques to control the difference between the two frequencies have been developed which depend solely upon the locations of the standard laser components and the spacing between the several glass flats which serve as one end mirror. The two laser beams have been intersected in flint glass to beat electrostrictively and produce intense, pulsed acoustic beams at 500 megahertz. The value of the method lies in its potential of producing much higher intensities and frequencies than do the conventional piezoelectric transducers.

TABLE OF CONTENTS

ACKNOWLEDGEMENTS

The support and assistance of many individuals and organizations have made possible the progress which it is hoped that this report represents. A few of these to whom the author is indebted are:

Prof. E.C. Crittenden, Jr., who conceived the project and has guided its development with careful thought and thoughtfulness.

Dean C.E. Menneken, who has provided crucial administrative support.

The Office of Naval Research for financial support.

The able technicians of the Machine Facility and the Department of Physics for construction of apparatus.

My wife, Lenore, for her patience and encouragement.

I. INTRODUCTION

In 1922 Leon Brillouin[1] predicted that if a light beam were passed thru an acoustic wave at the proper angle, part of the light would be diffracted at a discrete angle. By 1933 Brillouin[2] as well as others[3] had observed the diffraction at precisely the predicted angle. Brillouin had then begun to suspect that the frequency, as well as direction, of the light was shifted, but in his theoretical analysis considered the velocity of the sound wave as negligible compared with the light wave velocity, and lost the Doppler shift. That the light wave frequency was shifted, and by approximately the acoustic frequency, was found by Ali[4] in 1936. A precise experimental determination that the light frequency was shifted by exactly the acoustic frequency was made in 1963 by Cummins and Knable[5] but not until they had a laser available as the light source.

Brillouin scattering, as the term is now used, consists of the diffraction and Doppler shifting of a beam of light by an acoustic wave in a liquid or solid. The acoustic wave can be merely the thermal sound within the interaction medium or it can be an externally excited coherent wave. The angle which the light beam must make with the acoustic wave fronts was shown by Brillouin to correspond to Bragg's rule, with the wave fronts taking the role of the crystal lattice planes. It has since been shown that the analogy to Bragg reflection holds exactly only for an observer moving with the acoustic wave. In the fixed frame, the angles of incidence and reflection are slightly distorted and the Doppler shift appears. If the incident light falls at Bragg's angle on

the receding side of the acoustic waves, the Doppler shift as measured by Cummins is negative. Moreover, as verified experimentally by Korpel, Adler and Alpiner[6] in 1964, the amplitude of the acoustic wave is increased. If, on the other hand, the light falls on the advancing side of the acoustic waves, the Doppler shift is positive, while the acoustic amplitude, as observed by Korpel, is attenuated.

The inverse of the traditional Brillouin scattering, intersecting two light waves of slightly different wave lengths in an electrostrictive material to generate a sound wave, was demonstrated in 1964 by Korpel. Korpel and subsequently Caddes, Quate and Wilkinson[7] and others intersected, as shown in Figure (1-1), a giant pulse ruby laser beam with an externally excited acoustic wave in a solid or liquid to produce light shifted in frequency from the original laser output by Brillouin scattering.

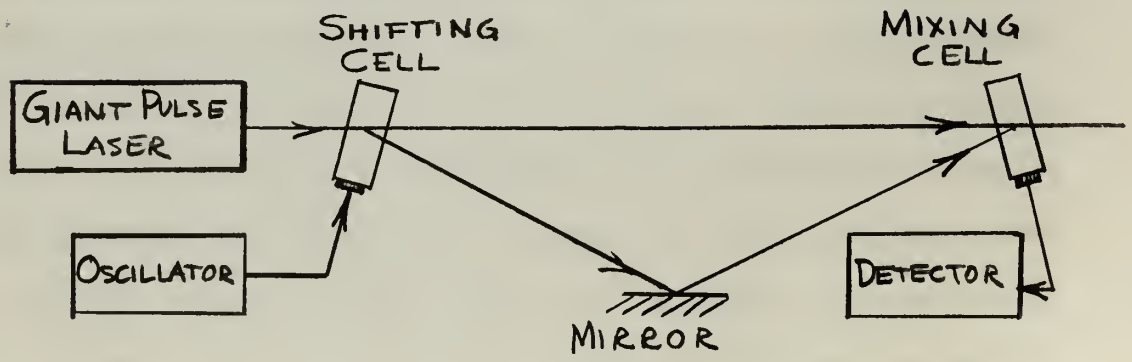

Figure 1-1. Brillouin Scattering Followed by Electrostrictive Beating

The weak, frequency-shifted beam was then re-intersected in an electrostrictive material with the original laser beam. Correct choice of the material in which the two beams intersected and correct choice of the angle between them resulted in an acoustic wave being produced in a unique direction and with frequency equal to the beat between the frequencies of the two light waves.

As Caddes commented, generation of hypersound by the inverse of Brillouin scattering, or electrostrictive mixing, makes it possible to generate acoustic waves at a desired position within the bulk of a transparent material. However the dependence upon stimulated Brillouin scattering for the generation of the shifted light beam is a severe limitation, again as suggested by Caddes. The method of Korpel and of Caddes does not provide a primary source of acoustic power, being limited to the same frequencies and even lesser intensities than otherwise required in the apparatus from a conventional electro-acoustic transducer.

A significant advancement toward making electrostrictive beating a useful research tool would be afforded by developing a procedure for generation of the frequency shifted beams which did not require scattering by the frequency which is ultimately desired. With this goal we have considered the following alternative means of generating the two light beams at slightly and controllably different frequencies.

1. Use of an intercavity Brillouin cell of the type reported by Siegman et.al.[8] Siegman placed a quartz or rutile crystal which was excited by a re-entrant cavity and transducer in the optical path between the active lasing medium and one end mirror, with both

end mirrors being totally reflective. Having the cell inside the laser cavity significantly increased the intensity of light available for scattering and frequency shifting. Moreover, because the unshifted laser light was passing through the cell with both a positive and a negative sense, light was scattered out with both positive and negative doppler shifts. If one were to beat the two scattered waves electrostrictively, sound would be produced with twice the frequency of that required in the Brillouin cell.

2. Use of two identical lasers, one at room temperature, the other cooled to slightly shift the positions of the energy levels in the lasing medium, and thus the center of the lasing fluorescent line. Our experience has indicated that while it is possible to cause lasing in some single, narrow mode, it is not possible, with available techniques, to determine precisely which mode will lase. This would produce an intolerable uncertainty in the beat frequency, and probably defeat this approach.

3. Single sideband suppressed carrier modulation of a laser beam as done in KDP by Buhrer et.al.,[9] to provide one beam, while the original laser output provides the other. A limitation on the flexibility of this procedure is imposed by the narrow bandwidth of the modulator. A 9.25 Gigahertz modulator constructed by Kaminow[10] was tunable over only 60 Megahertz. Until a light modulator can be built in which microwave velocity and light velocity are matched over a broader band, this method will be too limited in the range of frequency unless many different modulator cavities are built.

4. Splitting the laser beam into two parts and Doppler shifting the wavelength of one or both parts by means of a moving mirror. This method would make efficient use of the laser output, allow any desired partition of power between the two parts, and permit continuous change of the acoustic output frequency by simply changing the velocity of the Doppler shifting mirror. This was the first procedure attempted and is reported in Appendix B. It was not successful, however, presumably because of an incompatibility between the Doppler shifting machine and the laser used.

5. Use of a pair of longitudinal modes of the same laser. In 1966 Caddes referred to the use of "two laser modes" but did not specify two adjacent longitudinal modes nor did he give amplifying suggestions on how the procedure might be carried out. For longitudinal modes the difference in frequency, f, would be determined by $f = \frac{mc}{2L}$ where L is the effective length of the laser cavity and m the order of separation of the two modes. This approach becomes chiefly a laser mode control experiment where the problem, as dealt with by Hercher[10], of insuring lasing in only one spectrally narrow mode becomes the problem of insuring lasing in two or more spectrally narrow modes with a predictable and precise frequency separation. This procedure has manifest advantages in the simplicity of the apparatus over the alternatives 1 through 4 above. Production of intense 500 MHz acoustic pulses in solids by this pair of modes procedure for electrostrictive light beating is the subject of this report.

II. QUALITATIVE THEORY

The electrostrictive mixing of two light waves when merged at the proper angle to generate an acoustic wave at the beat frequency can be described by a straight forward analysis which is appealing in its simplicity. The results which this yields when interpreted by the quantum theory, are in comforting accord with basic concepts. Agreement with a relativistically corrected description of Bragg reflection can be easily shown.

Electrostrictive Mixing of Two Light Waves

In a piezoelectric material, the elastic strain, $\vec{u}$, can be related to the electric field $\vec{E}$, thru a phenomenological inverse piezoelectric tensor $\vec{\alpha}$ by,

$$u_i = \alpha_{ij} E_j \tag{2-1}$$

If the material is also electrostrictive and manifests a strain proportional to the square of the electric field, an additional term must be included to reflect this property. The tensor representation of the strain produced by the electric field then becomes

$$u_i = \alpha_{ij} E_j + \beta_{ijk} E_j E_k \tag{2-2}$$

While the piezoelective effect has been exhaustively studied and applied since its discovery by the Curie brothers Jacques and Pierre in 1880, the electrostrictive effect has only recently become of interest. At the moderate electric field strengths which were available for experimentation prior to the advent of the giant pulse laser, the linear piezoelectric effect completely masked the much smaller quadratic electrostrictive effect, thus

its long obscurity. But when the electric field is sufficiently strong, the quadratic term becomes noticable in some materials and indeed is dominant in the interaction here discussed.

If we have two monochromatic, coherent, light waves of different frequencies traversing a region, we can write the associated electric field as

$$E = \vec{E}_1 \cos(\omega_1 t - \vec{k}_1 \cdot \vec{r}) + E_2 \cos(\omega_2 t - \vec{k}_2 \cdot \vec{r} + \varphi_2) \qquad (2\text{-}3)$$

The strain induced by this field in the interaction medium is then given, including both piezoelectric and electrostrictive effects, by

$$\begin{aligned} u_i = {} & \alpha_{ij} E_{1j} \cos(\omega_1 t - \vec{k}_1 \cdot \vec{r}) + \alpha_{ij} E_{2j} \cos(\omega_2 t - \vec{k}_2 \cdot \vec{r} + \varphi_2) \\ & + \beta_{ijk} E_{1j} E_{1k} \cos^2(\omega_1 t - \vec{k}_1 \cdot \vec{r}) + \beta_{ijk} E_{2j} E_{2k} \cos^2(\omega_2 t - \vec{k}_2 \cdot \vec{r} + \varphi_2) \\ & + 2\beta_{ijk} E_{1j} E_{2k} \cos(\omega_1 t - \vec{k}_1 \cdot \vec{r}) \cos(\omega_2 t - \vec{k}_2 \cdot \vec{r} + \varphi_2) \end{aligned} \qquad (2\text{-}4)$$

Note that the symmetry of the electrostriction tensor $\vec{\beta}$, $\beta_{ijk} = \beta_{ikj}$, has been invoked. The last term in this strain expression can be written

$$\beta_{ijk} E_{1j} E_{2k} \left\{ \cos[(\omega_1+\omega_2)t - (\vec{k}_1+\vec{k}_2)\cdot\vec{r} + \varphi_2] + \cos[(\omega_1-\omega_2)t - (\vec{k}_1-\vec{k}_2)\cdot\vec{r} - \varphi_2] \right\} \qquad (2\text{-}5)$$

If the angle between $\vec{k}_1$ and $\vec{k}_2$ is adjusted so that

$$|\vec{k}_1 - \vec{k}_2| = \frac{\omega_1 - \omega_2}{v_s} \qquad (2\text{-}6)$$

where v_s is the speed of sound of angular frequency

$$\omega_s = \omega_1 - \omega_2 \qquad (2\text{-}7)$$

then the last half of equation (2-5) represents an acoustic wave excited in the material. All other terms from equation (2-4) are either static strains or are elastic strain excitations traveling at velocities of approximately the speed of light. Hence the elastic strain excited in any infinitesimal region, as it propagates at the acoustic velocity through a neighboring region, finds itself out of phase with the strain which is electrostrictively excited there. Thus the electrostrictive effect couples the two incident light waves and produces an acoustic wave of the form

$$\cos\left[(\omega_1-\omega_2)t-(\vec{k}_1-\vec{k}_2)\cdot\vec{r}\right] = \cos\left(\omega_s t-\vec{k}_s\cdot\vec{r}\right) \qquad (2\text{-}8)$$

but no other acoustic waves.

Multiplying Equation (2-7) by Planck's constant gives,

$$\hbar\omega_1 = \hbar\omega_2 + \hbar\omega_s \qquad (2\text{-}9)$$

Similarly the other identity implicit in Equation (2-8)

$$\vec{k}_1 = \vec{k}_2 + \vec{k}_s, \qquad (2\text{-}10a)$$

becomes

$$\hbar\vec{k}_1 = \hbar\vec{k}_2 + \hbar\vec{k}_s \qquad (2\text{-}10b)$$

These suggest that we consider the interaction of equal numbers of photons at ω_1, photons at ω_2 and phonons at ω_s. Both energy and momentum are conserved, but unexpectedly, while the ω_1 light wave is absorbed the ω_2 radiation plays only a catalytic role.

Relativistic Validity of $\omega_1 = \omega_2 + \omega_s$

The very simple relationship of Equation (2-7) between the frequencies of the incident light waves and the generated acoustic wave is exact even for high acoustic velocities. It will now be

shown that the relativistic correction is implicit in the foregoing derivation. The similarity of stimulated Brillouin scattering with Bragg reflection, the evenly spaced layers of contraction in the acoustic wave corresponding to the crystal lattice layers, suggests an alternative derivation paralleling the Bragg reflection law.

The relationships of conventional Bragg reflection by the layers of a regular lattice, stationary with respect to the observer, are easily seen from inspection of Figure (2-1). If Rays a and b are parts of an incoming plane wave, the condition of constructive interference requires that the distance efg be an integral number, m, of wave lengths yielding

$$m\lambda_1 = 2d \sin\theta_1 \qquad (2\text{-}11)$$

where λ_1 is the wavelength of the incoming wave and also of the outgoing wave, d the crystal lattice layer spacing and θ_1 the angle between either the incoming or the reflected ray and the layers.

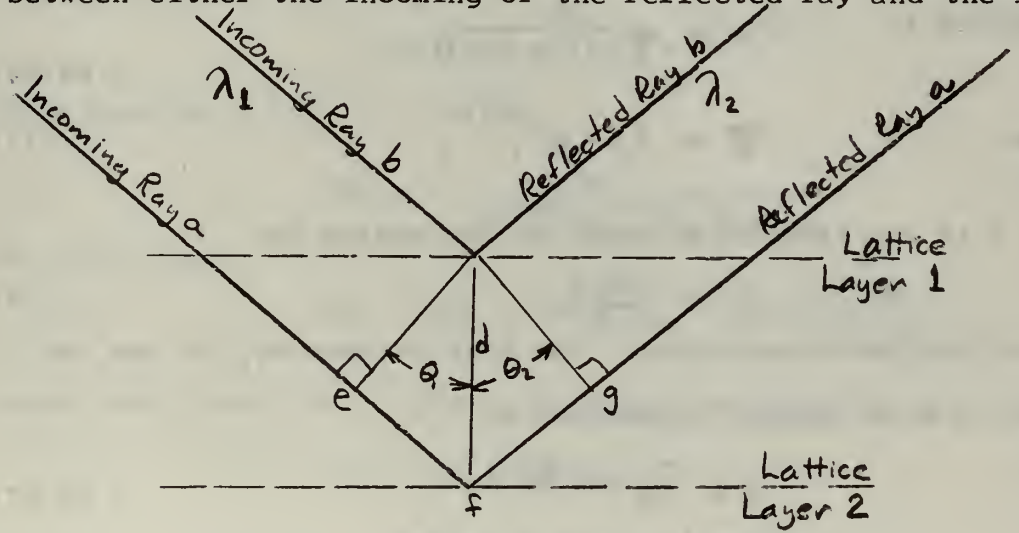

Figure (2-1). Bragg Reflection

Equation (2-11) can be corrected relativistically and shown to lead to Equation (2-7) by rewriting (2-11) for the case of the lattice layers moving at v_s, the acoustic wave velocity. An observer traveling along at v_s with the acoustic wave still sees the same relations which led to Equation (2-11), now denoting the quantities as seen in the moving frame with primes.

$$m\lambda_1' = 2d'\sin\theta_1' \tag{2-12}$$

In this moving frame we still have

$$\lambda_1' = \lambda_2' \tag{2-13a}$$

$$\theta_1' = \theta_2' \tag{2-13b}$$

and $$\omega_1' = \omega_2' \tag{2-13c}$$

but when these quantities are transformed back to a fixed frame, the equalities fail. The incoming wave length transforms[12] according to

$$\lambda_1' = \frac{\lambda_1}{\gamma(1-a\sin\theta_1)} \tag{2-14}$$

where

$$\gamma = (1-a^2)^{-1/2}, \tag{2-15}$$

n is the refractive index of the medium and

$$a = \frac{v_s n}{c} \tag{2-16}$$

is defined for convenience. The lattice spacing, or now the acoustic wave length, transforms by

$$d' = \lambda_s' = \gamma\lambda_s \tag{2-17}$$

Also

$$\sin\theta_1' = \frac{\sin\theta_1 - a}{1-a\sin\theta_1} \tag{2-18}$$

Substituting Equations (2-14), (2-17) and (2-18) into (2-12) yields

$$\lambda_1 = 2\lambda_s\gamma^2(\sin\theta_1 - a) \tag{2-19}$$

written in quantities measurable in the fixed frame. (This equation is not needed to derive Equation (2-7)).

The reflected wavelength can be transformed by

$$\lambda_2' = \frac{\lambda_2}{\gamma(1 + a \sin\theta_2)} \tag{2-20}$$

Combining Equations (2-13a), (2-14) and (2-20) yields

$$\omega_2 = \omega_1 \left(\frac{1 - a \sin\theta_1}{1 + a \sin\theta_2} \right) \tag{2-21}$$

where ω_2 is the reflected wave angular frequency and ω_1 is the incident wave angular frequency, both in the stationary frame. The sine of the angle of reflection transforms by

$$\sin\theta_2' = \frac{\sin\theta_2 + a}{1 + a \sin\theta_2} \tag{2-22}$$

Substituting Equations (2-18) and (2-22) into (2-13b) yields

$$\sin\theta_2 = f(a, \sin\theta_1) \tag{2-23}$$

From Equation (2-19) we can get

$$\omega_1 = \frac{\omega_s}{2\gamma^2 a(\sin\theta_1 - a)} \tag{2-24}$$

We now write

$$\omega_1 - \omega_2 = \omega_1 \left(1 - \frac{1 - a\sin\theta_1}{1 + a\sin\theta_2} \right), \tag{2-25}$$

substitute Equations (2-24) and (2-23) and simplify yielding

$$\omega_1 - \omega_2 = \omega_s. \tag{2-7}$$

Relativistic Validity of $\vec{k}_1 = \vec{k}_2 + \vec{k}_s$

Verification that Equation (2-10a), showing conservation of momentum for scattering of a single photon, contains the relativistic correction can also be done using the relations above which

describe Bragg scattering by an acoustic wave. Rearranging Equation (2-21) yields

$$\omega_1(1-a\sin\theta_1) = \omega_2(1+a\sin\theta_2) \tag{2-26a}$$

$$\frac{1}{a}(\omega_1-\omega_s) = \omega_1\sin\theta_1 + \omega_2\sin\theta_2 \tag{2-26b}$$

Substituting Equation (2-16),

$$\frac{\omega_s}{v_s} = k_s = k_1\sin\theta_1 + k_2\sin\theta_2 \tag{2-27}$$

The cosine of the angle of the incoming wave transforms by

$$\cos\theta_1' = \frac{\cos\theta_1}{\gamma(1-a\sin\theta_1)} \tag{2-28}$$

and similarly the cosine of the angle of reflection transforms by

$$\cos\theta_2' = \frac{\cos\theta_2}{\gamma(1+a\sin\theta_2)} \tag{2-29}$$

Equating the right hand sides of Equations (2-28) and (2-29) by Equation (2-13b) and multiplying the right and left respectively of Equation (2-26a) yields

$$\omega_1\cos\theta_1 = \omega_2\cos\theta_2 \tag{2-30}$$

Substituting $\omega_i = \frac{k_i c}{n}$ we have

$$k_1\cos\theta_1 = k_2\cos\theta_2 \tag{2-31}$$

Scalar Equations (2-27) and (2-31) are sufficient to show the vector equality

$$\vec{k}_1 = \vec{k}_2 + \vec{k}_s \tag{2-10a}$$

as shown in Figure (2-2).

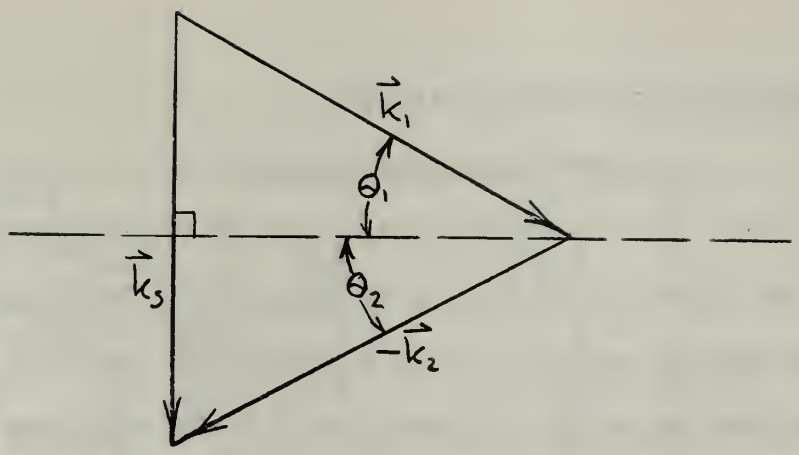

Figure (2-2). Vector diagram showing conservation of momentum

Thus both the relationship between frequencies showing energy conservation in a single photon-phonon interaction and the vector equation showing momentum conservation, as derived from the wave equations, are shown to also be the result of a relativistic treatment as a Bragg reflection.

III. DESCRIPTION OF THE APPARATUS

The Q-switched Laser

The ruby laser with bleachable dye Q-switch, apertures for control of transverse modes, a roof prism for the rear reflector, and a three-flat resonant front reflector is shown in Figure III-1.

The roof prism was of fused quartz with surfaces flat within 1/20 wavelength and geometry to assure the exiting ray parallel with the entering ray within one second of arc.

The bleachable dye cell walls were of optical crown glass. The cell measured ten millimeters thick inside with walls two millimeters thick. Flatness and parallelism were sufficient to show no fringes in reflection over a one centimeter aperture. A ground glass stopper prevented evaporation of the solvent and absorption of water vapor. Cryptocyanine dye was dissolved in methyl alcohol and diluted empirically to give the desired threshold of lasing. The cell was oriented at Brewster's angle to allow lossless transmission of light with horizontal E-vector.

The aperture used to restrict transverse modes was a light gauge sheet of brass with two holes four millimeters in diameter, spaced five millimeters center to center. The aperture was oriented with one hole vertically above the other.

The ruby measured three inches long by 3/8 inch diameter with the ends cut at Brewster's angle, parallel within 5 seconds of arc, and flat within one-tenth wavelength. The doping was 0.05% by weight of chromium oxide. The optical quality was specified in purchasing the crystal by requiring that it show two or fewer fringes when examined in a two-pass Twyman Green interferometer.

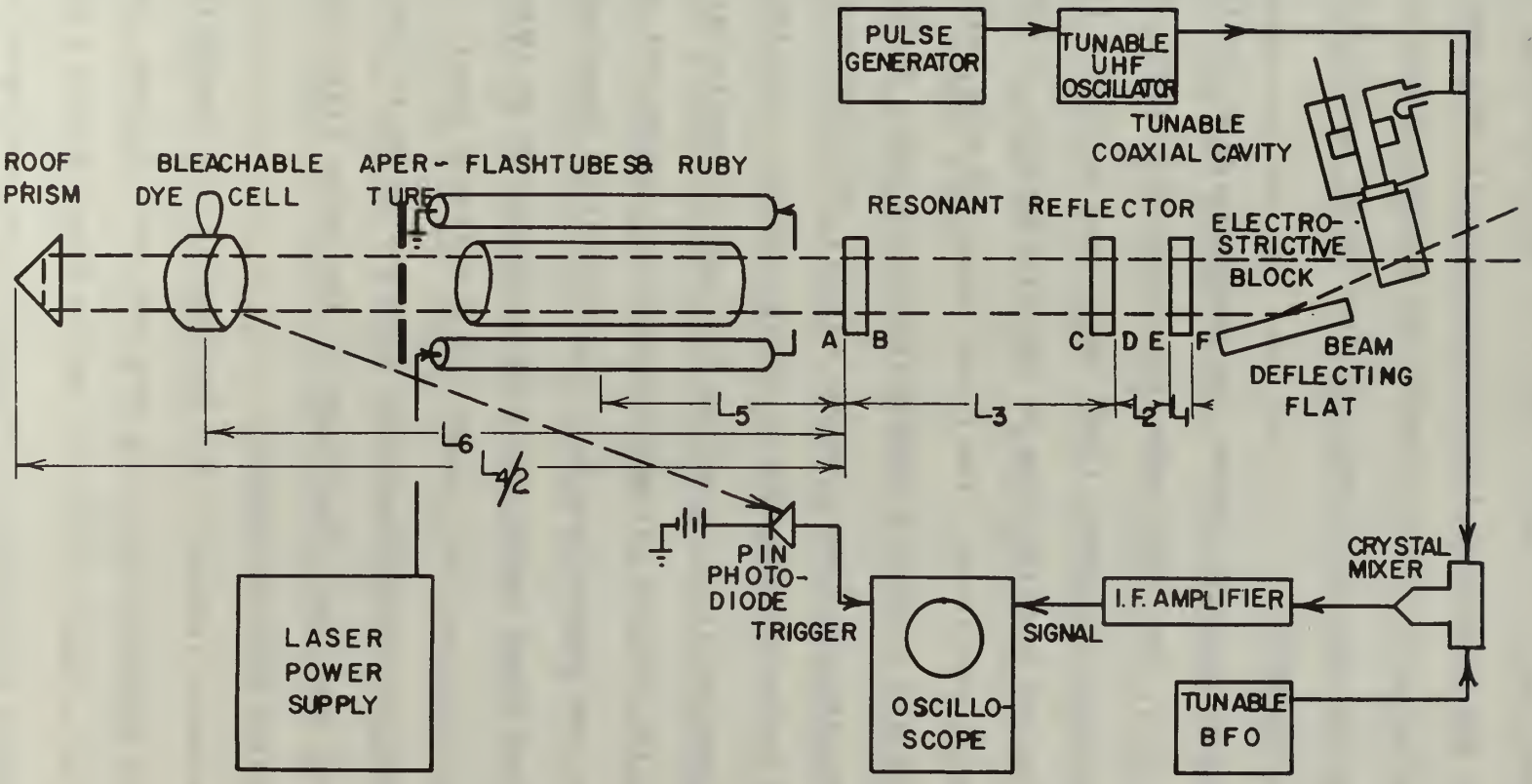

FIGURE III-1

SCHEMATIC DIAGRAM OF APPARATUS

OPTICS SHOWN IN SIDE VIEW

It is not known that the crystal met this specification. The crystal axis was 60 degrees from the cylindrical axis and in a plane perpendicular to that in which the Brewster's angle was measured, so that the preferred polarization of emission was not reflected at the ends.

The optical pumping chamber was manufactured by Optics Technology, Inc., for their model 130 Q-switched laser. Two twelve centimeter long xenon flash tubes, one above the ruby and one below, spaced from the ruby by two millimeters, provided the optical pumping radiation. The flash tubes and ruby, with a soft glass ultraviolet absorbing shield around the ruby, were enclosed in a machined and polished aluminum cavity. The aluminum cavity was a round cornered rectangle in cross-section. Cooling air entered through axial slits beside the ruby and exited at the open ends. The cooling air was filtered to remove dust and cooled to or below room temperature by a tap water heat exchanger.

The laser power supply was also manufactured by Optics Technology, Inc., for their model 130 Q-switched laser. An eight hundred microfarad capacitor bank stored up to 2500 joules at 2500 volts which was discharged to the xenon flash tubes through a pulse forming ladder.

The resonant reflector was designed to, in conjunction with longitudinal positioning of the dye cell and the ruby, induce lasing in two or more spectrally narrow modes having a precise and predictable difference in wavelength, or correspondingly in frequency.

Physically, the resonant reflector consisted of three optically dense (Index of refraction 1.75) flats as shown in Figure III-1. Surface B and C were evaporatively coated with one quarter wavelength of magnesium fluoride to reduce reflection; surfaces A, D, E and F were uncoated. All surfaces were flat within one tenth wavelength and flat EF, with both surfaces uncoated, had a wedge of less than two seconds of arc. Flats CD and EF were spaced and held parallel by a short length of fused quartz tubing and the assembly mounted in a gimbal mount with micrometer screws to control two degrees of rotation. Flat AB was separately mounted in another gimbal mount.

The phenomenon upon which the design of the resonant reflector was based was the periodic variation with wavelength in the total reflectivity of two or more parallel partially reflective surfaces. Appendix A deals with the analysis of resonant reflectors in general and in particular deals with analysis of the four surface resonant reflector which was used. Referring to Figure III-2, if the optical pumping is sufficiently intense, the required mirror reflectivity will be low and lasing can occur at the wavelengths of many of the local maxima. If the optical pumping intensity is carefully reduced, fewer and fewer of the local maxima will be of sufficiently high reflectivity and finally lasing will occur at the wavelength of only one of the narrow maxima.

The spacings L_1, L_2 and L_3 as shown in Figure III-1 were selected as follows:

L_1, the effective optical thickness of a dense flat that was on hand was 0.566 cm so that the reflectivity of flat EF

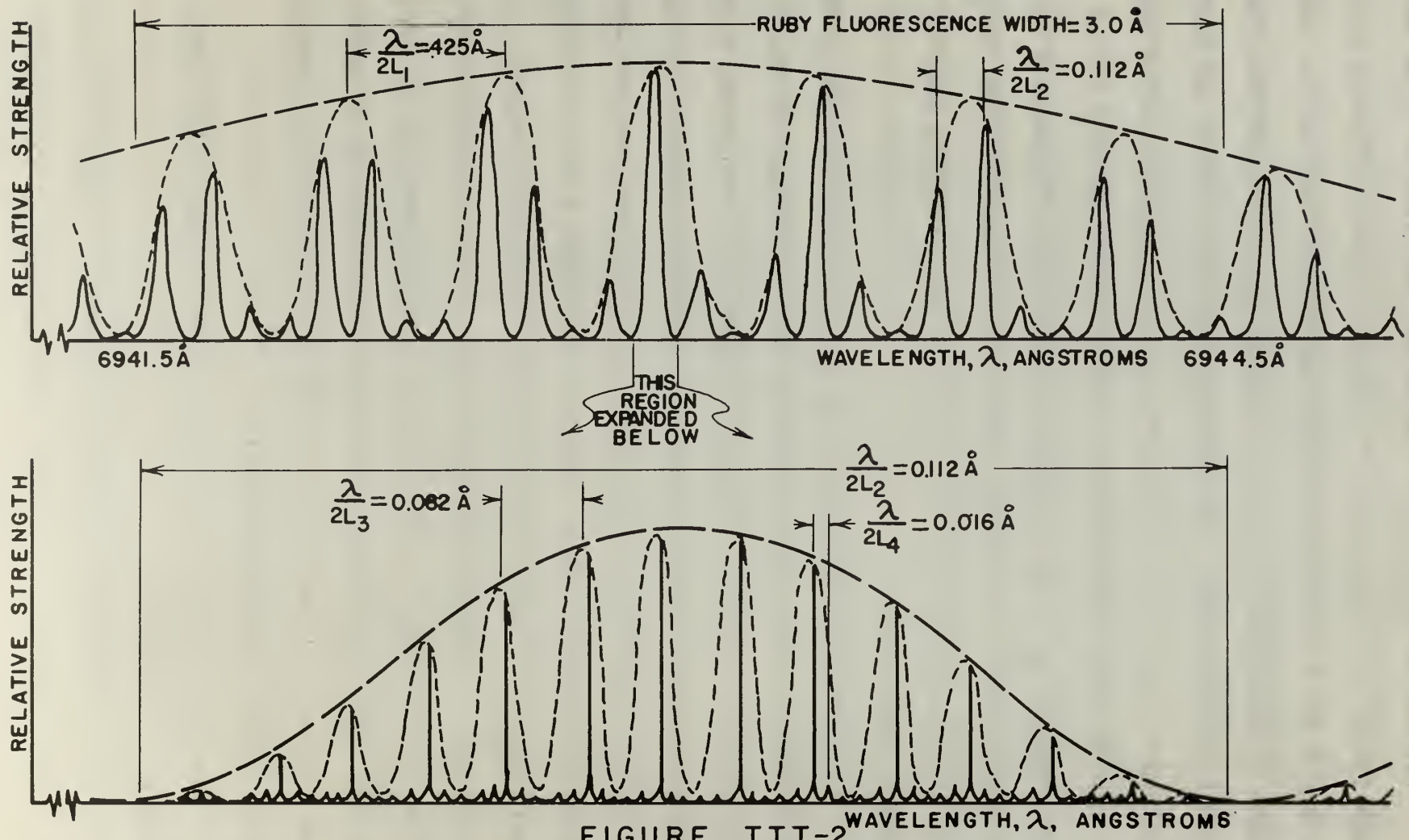

FIGURE III-2

VARIATION VERSUS WAVELENGTH OF THE RELATIVE STRENGTH OF LONGITUDINAL MODES CAUSED BY WAVELENGTH SELECTIVITY IN THE GAIN OF THE RUBY AS WELL AS IN THE FEEDBACK LOSSES

by itself was a comb like Figure A-1a with maxima separated by

$$\Delta\lambda = \frac{\lambda^2}{2L_1} = 0.425\ \text{Å}$$

Or equivalently the maxima are separated in frequency by

$$\Delta f = \frac{c}{2L} = 26.5 \text{ Gigahertz}$$

This gave only seven maxima of the comb due to L_1 within the 3Å ruby fluorescence line width so that the central one of these maxima had sufficiently higher reflectivity than its neighbors to be the only one in which lasing occured. Of course it may happen for a given L_1 that the center of the emission line is such that two reflectivity maxima straddle the peak; one would then have to fire the laser again, warming the ruby and shifting the emission line center. In early tests of the laser, using a single flat of thickness L_1 interferograms were produced by a Fabry-Perot étalon with a spacing of one centimeter and were photographically recorded. Even with a resolution no better than about 0.02Å, two different wavelengths were sometimes observed.

L_2, the length of the eighteen millimeter diameter fused quartz tube, was 2.215 centimeter so that surfaces E and D alone produced a comb like Figure A-1a with maxima spaced by $\Delta\lambda = 0.110$Å or in frequency by $\Delta f = 6.77$ GHz. Surface D in conjunction with both surfaces of the first flat, E and F, produced a comb like Figure A-1b where each of the envelope lobes contained four local maxima. Surface C was

anti-reflective coated so did not influence the comb. The wavelength at which lasing could occur was thus confined to the peak of a single 0.110Å wide lobe.

L_3, the spacing of surface A of the separately adjustable flat from surface D of the triple reflector was chosen by

$$L_3 = \frac{c}{2f_s} \qquad (3\text{-}1)$$

where f_s was the frequency of sound desired. The frequencies of sound desired were in the neighborhood of 500 MHz giving spacings L_3 in the neighborhood of 30 centimeters. The variation of reflectivity versus wavelength for surface A, D, E and F was then as shown in Figure A-1c where only four peaks of the comb due to L_2 lay in each lobe of the comb due to L_1, but fourteen peaks of the comb due to L_3 lay within each lobe of the comb due to L_2. As shown in Figure 3-2, only seven peaks of the envelope of the reflectivity variation lay within the ruby omission line width. Thus a certain margin of optical pumping intensity above threshold which was insufficient to cause lasing at the wavelength of more than one peak of any of the other combs was sufficient to cause lasing at more than one peak of the comb due to L_3. The frequency difference between the emissions of these adjacent modes was the desired 500 Megahertz.

That Equation (3-1) is correct to give the separation between peaks of a reflectivity versus frequency comb can be shown by substituting Equation (A-4) in

$$f = \frac{c}{\lambda}, \quad \Delta f = -\frac{c}{\lambda^2}\Delta\lambda \qquad (3\text{-}2)$$

to obtain $$\Delta f = \frac{c}{2L}$$

or rearranging $$L = \frac{c}{2\Delta f} \qquad ((3\text{-}3)$$

In the above equations, f is frequency, c the speed of light, λ light wave length, Δf the difference in frequency between two subsequent longitudinal modes for a given resonator length, and L the effective length of the resonator.

The cavity length, L_3, of about 30 cm was not sufficient to contain all of the components required within the laser cavity. By selecting the overall length of the laser, L_4, to be an integral prime multiple of the critical length, L_3, it was possible to avoid disturbing the phenomenon of multiple longitudinal modes of L_3 lasing simultaneously. The smallest prime integer which allowed sufficient room within the cavity was 5, or $L_4 = 5L_3$. The importance of the multiple being not only integral but prime is explained below. As shown in Figure III-2 the gross, meaning not to a precision of a fraction of a wavelength, ratio of L_4 to L_3 gave exactly five peaks of the comb of reflectivity due to L_4 within each lobe of the comb due to L_3. Thus the central or highest peak of the comb due to L_4 occupied the same position relative to center within each of the lobes of the comb due to L_3. Here one can see why it was necessary that L_4 be an integral multiple of L_3. However, L_4 was not controlled to be five times L_3 within a precision of a part of a wavelength, so the situation was probable of there existing no wavelength within the width of the selected lobe of the comb due to L_2 for which both L_3 and L_4 were an integral number of half wave lengths. Therefore within each of the lobes due to

L_3 there could have been, instead of one peak of the comb due to L_4 at the center and distinctly higher, a pair of peaks of the comb due to L_4 straddling the center and of comparable peak reflectivity. Assurance that, in this eventuality, lasing would not occur in the left of center peak within one lobe of the comb due to L_3 and in the right of center peak within the next lobe, was given by judicious positioning of the ruby laser rod and the bleachable dye cell within the length $L_4/2$.

L_2, the position of the ruby laser rod, was selected to encourage lasing in every fifth longitudinal mode of the optical resonator of length L_4 by the following rationale:

A given longitudinal mode of the cavity with length L_4, which may be called the nth order mode, is a standing wave with n antinodes and with nodes at the mirror surfaces and at every half wavelength in between. The next higher order longitudinal mode with n + 1 antinodes in the length L_4 and with wavelength shorter by $\Delta\lambda = \frac{\lambda^2}{2L_4}$ has its antinodes in coincidence with those of the nth mode only near the end mirrors. Near the midpoint of the cavity, $L_4/2$ from either end, the antinodes of the n + 1st mode coincide with the nodes of the nth mode. Similarly the second higher order mode with n + 2 antinodes in L_4 has its antinodes in coincidence with those of the nth mode near both mirrors and near $L_4/2$. Finally, the n + 5th order mode has its antinodes in coincidence with those of the nth order mode, or the two modes could be said to be in phase in space, near the end mirrors and near p $L_4/5$ where p is an integer between

zero and four. At $(p + \frac{1}{2})L_4/5$ the antinodes of the n + 5th mode coincide with the nodes of the nth node, or the two modes could be said to be out of phase in space. It can be seen that if a pair of modes differ by a prime number of half wavelengths then the regions of constructive as well as of destructive interference are unique in the sense of being common to no pair with lower order separation. This is why L_4 was chosen as a prime multiple of L_3.

Lasing in the nth, n + 5th, and n + 10th etc., longitudinal modes, or equivalently, lasing in the nth and n + 5mth order longitudinal modes was encouraged by placing the ruby where the standing waves of the different modes were out of phase in space so that they stimulated different regions of ruby and did not compete for energy from the excited ions. By choosing $L_5 = L_4/10$, the n + 5mth mode of the cavity L_4 was encouraged to lase with the nth mode, while the n + 1st thru n + 4th and n + 6th thru n + 9th etc., were discouraged.

Following arguments similar to those used to locate the ruby, the dye cell was positioned at $2\ L_4/5$. In this region, the nth and n + 5mth modes were in phase in space so the preferred modes co-operated by the nth mode, bleaching antinode regions which were common to all the n + 5mth modes. The n + 1st thru n + 4th and n + 6th thru n + 9th etc., modes were not in phase in space with the nth mode at the location of the cell, hence their emission simultaneously with the nth mode was not encouraged.

The arrangement of the optical components of the laser caused the laser light to be emitted as a pair of intense, parallel, highly collimated beams with a diameter of about 2 millimeters and a spacing of about 4 millimeters. Having the laser output in this form was most convenient because it allowed the necessary two beams of light to be merged at the required angle, permitted a short optical path from the laser to the electrostrictive medium, and obviated the use of a beam splitter.

During initial checkout of the Q-switched laser it was observed that when the flash cavity was oriented with the lamps in a plane perpendicular to the roof edge of the prism, lasing frequently occurred in two symmetrical millimeter spots, side by side in the plane of the flash lamps. The position of the spots corresponded to the diffuse focii within the ruby of the optical pumping to light from the two linear flash tubes. The prism apparently acted to fold the emission of one of the focii into the other. Rotating the ruby so that its preferred emission polarization was perpendicular to the pumping rays directly from the flash tubes was observed to enhance the "pair of spots" lasing mode. The double aperture was designed with the holes of the diameter and spacing which was found to best confine lasing to the mode in which the lasing beam passed thru one of the pumping light focii in the ruby and then was folded back to pass thru the other pumping light focus.

The polarization of the laser output was horizontal because of the preferred emission of the ruby with the flash lamps positioned over and under, the orientation of the ruby crystal

axis which was 60° from the cylindrical axis and in a vertical plane, the orientation of the Brewster's angle ends of the ruby, and the orientation of the dye cell at Brewster's angle, measuring in the horizontal plane.

Optics External to the Laser

The lower limb of the double spot laser output was reflected to intersect the upper limb in the electrostrictive block by the beam deflecting flat shown in Figure III-1. The beam deflector was an uncoated glass flat 0.63 cm thick by 5.0 cm wide. The length of the flat used with a dense flint glass electrostrictive block was 11 cm. When doing the interaction in sapphire, the intersection angle was smaller, necessitating the use of a longer flat of length 18 centimeters. Flatness of the flats was poorer than one wavelength over the long aperature used. Support and positioning of the glass flats was by a kinematic count.

The electrostrictive block was inserted in the end of the tuned coaxial cavity which was held by a rigid aluminum mount having provision for translational adjustment in three directions and allowing fine adjustment of rotation in the plane of intersection of the two light beams.

All of the optical components were mounted on specially machined aluminum blocks which were clamped to the ways of a Gaertner 1.5 meter cast iron optical bench.

The Electrostrictive Material Blocks and Transducers

The first electrostrictive material used was a block of Schott F 1 flint glass. The index of refraction quoted by the supplier was n = 1.62077 at 6563Å and n = 1.61514 at 7682Å. Measurements of the block were six by ten by twenty millimeters

with all faces polished and flat within one quarter wavelength. Parallelism of the two six by ten millimter faces was specified to be within ten seconds of arc. The light beams were passed through in the ten millimeter direction and sound generated in the twenty millimeter direction.

Transducer coupling of the phonon energy in the flint glass, to the resonant coaxial cavity for detection was by a piezoelectric cadmium sulfide layer deposited on one of the six by ten millimeter end faces. The cadmium sulfide transducer was applied by Microwave Electronics Company of Palo Alto, California. The end of the block was first evaporatively coated with about 1000 Angstroms of chromium and then with one micron of gold. One electrode was thus provided by the gold layer while the other was mechanically positioned on the front side of the cadmium sulfide. The cadmium sulfide was applied in a 0.170 inch diameter spot with a thickness of two microns for a center frequency of about 500 megahertz. Band width was specified to be $\pm$ 20% and insertion loss was to be eight to fifteen decibels at mid-frequency. Acoustic loss in the flint glass was so high that precise measurement of the insertion loss was not accomplished, but it was found to be of the order of the specification. Strong frequency dependence of acoustic attenuation in the flint glass also made it difficult to check band width.

The electrostrictive mixing was also done in a block of synthetic sapphire of the same dimensions as the flint glass block. The crystal axis was specified to be within 0.5^{o} of the twenty millimeter dimension. Flatness of the six by ten millimeter faces

was specified to be within one tenth wavelength and parallelism within two seconds of arc. Flatness of the ten by twenty millimeter faces was specified to be within one quarter wavelength and parallelism within ten minutes of arc. The six by twenty millimeter faces were unpolished. The light beams were passed through in the six millimeter direction and sound generated in the twenty millimeter direction.

A quartz transducer was used to couple the generated phonons from the sapphire block to the tunable coaxial cavity. The quartz disc was cut with the x-axis parallel to the cylindrical axis, with such thickness as to give a fundamental resonance at ten megahertz, and with a diameter of 7/32 inch. The quartz had its 24th overtone at 490.5 MHz and its 25th at 510.5 MHz. One of the six by ten millimeter ends of the sapphire block was evaporatively coated with a few thousand Angstroms of aluminum which provided one electrode and the quartz bonded to the aluminum with Canada balsam. Insertion loss of the cavity and transducer together was measured to be 13 db while band width was less than 0.5 MHz.

The Tunable Coaxial Cavity

The high impedance of the electromagnetic field in the quartz transducer was matched to the 50 ohm coaxial transmission line by a tunable coaxial cavity. The design of the coaxial cavity followed the procedures and curves given by J.G. Stephenson[12]. Though Stephenson did not suggest use of his design for coupling to a piezoelectric transducer, the concentration of electric field across the gap under the end of the center post in his cavity made it ideal.

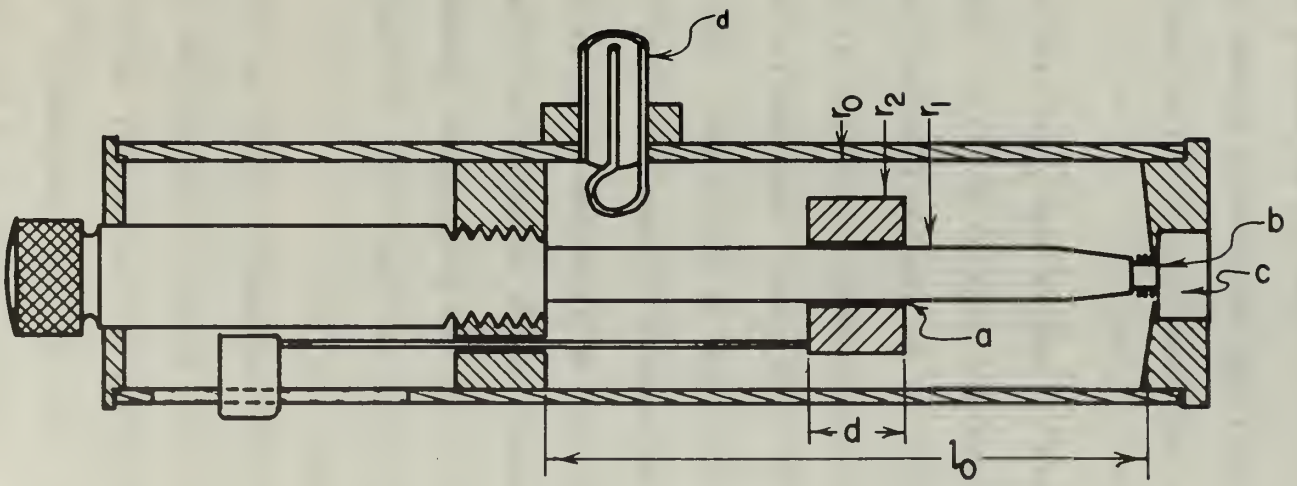

r_0 = 1.90cm.
r_2 = 1.53cm.
r_1 = 0.48cm.
d = 1.09cm.
l_0 = 11.30cm.

FIGURE III-3

THE TUNABLE COAXIAL CAVITY

The dimensions generated by Stephenson's design formulae and curves are shown in a cross sectional view in Figure III-3. Tuning of the cavity was provided by a sliding discontinuity on the center conductor. A tuning range of about 40 megahertz was possible. The tuning sleeve was insulated from the center conductor by a thin teflon sleeve at (a) in Figure III-3.

Intimate electrode contact with minimal danger of damage to the face of the delicate and expensive cadmium sulfide transducer was provided by the small metal bellows at (b) in Figure III-3. The diameter of the bellows was 0.156 inch and a force of 0.11 ounce was required to compress it 0.010 inch. The bellows had nine convolutions with a planar face to contact the transducer. The Servometer Corporation, Clifton, New Jersey, manufactured the bellows by electroplating a metal form with nickel, dissolving out the form and then electroplating gold over the nickel.

A rectangular recess in the end plate of the cavity at (c) in Figure III-3 accepted the block of electrostrictive material. Coupling out of the cavity was by a loop at (d) in Figure III-3 with a General Radio Type 874 connector attached. An adjustable short tuning stub inserted in the coaxial line at the output of the cavity further assisted in matching.

The Signal Detector

Detection of the signal from the crystal was accomplished by heterodyning and displaying the amplified I.F. envelope on an oscilloscope. The 500 MHz signal was beat down to 30 MHz in a General Radio model 874-MR crystal mixer. A continuous wave beat frequency was provided by a General Radio model 1209B unit oscillator tuned 30 MHz above the frequency which the resonant reflector

in the laser was adjusted to produce. Amplification of the crystal mixer output signal was accomplished by an LEL Inc., model IF 21 amplifier with six amplification stages synchronously tuned for narrow band width.

The pulses were displayed by feeding the envelope of the amplified IF signal to both vertical amplifiers of a Tektronix type 555 dual beam oscilloscope with two type L plug-in units. Use of a dual beam oscilloscope with different vertical gain factors allowed signals with a large uncertainty in amplitude to be displayed on readable scales. Triggering of the oscilloscope was by a Hewlett-Packard type 4205 PIN photodiode which was illuminated by the laser light reflected from the surface of the dye cell. The photodiode had a rise time much less than the several nanosecond buildup time of the Q-switched laser pulse and gave a pulse magnitude of a few volts when reverse biased at 30 volts. Assurance that the oscilloscope sweep did not trigger on the optical pumping flash was given by raising the trigger threshold on the oscilloscope and by shielding the photodiode from direct illumination by the pumping light which spilled out the ends of the optical pumping chamber.

In the final and most conclusive data trials, one channel of the type 555 oscilloscope was used to display the photodiode signal on the same time base as the detector output. The photodiode signal was also displayed on a Tektronix type 519 oscilloscope with a travelling wave cathode ray tube. This oscilloscope had more than adequate frequency response to show the 500 MHz beat produced in the photodiode signal when its illumination contained light of two frequencies differing by 500 MHz.

IV. PROCEDURE

Optical Alignment

Alignment of the laser optical components, the lower beam reflector, and the electrostrictive block was found to be critical. Small errors resulted in no sound pulse being produced, with seldom a direct indication of the correction required. The very slow repetition rate of firing the laser (one pulse every two minutes), imposed principally by slow dissipation of heat from the ruby, made it impossible to align the optics by simply observing changes in output while adjusting.

A small helium-neon continuous wave laser with an output power of about 0.3 milliwatts in a one millimeter beam with a divergence of less than one milliradian was the principal alignment tool. The alignment laser was positioned along side the Q-switched laser and its beam reflected to go back down the axis of the Q-switched laser as shown in Figure IV-1, with a total path length of ten meters. At ten meters the gas laser beam had diverged to one centimeter, the largest spot which could be accomodated through the optical components. The reflections from the resonant reflector and prism were then displayed on a white screen having a one millimeter hole in front of the gas laser.

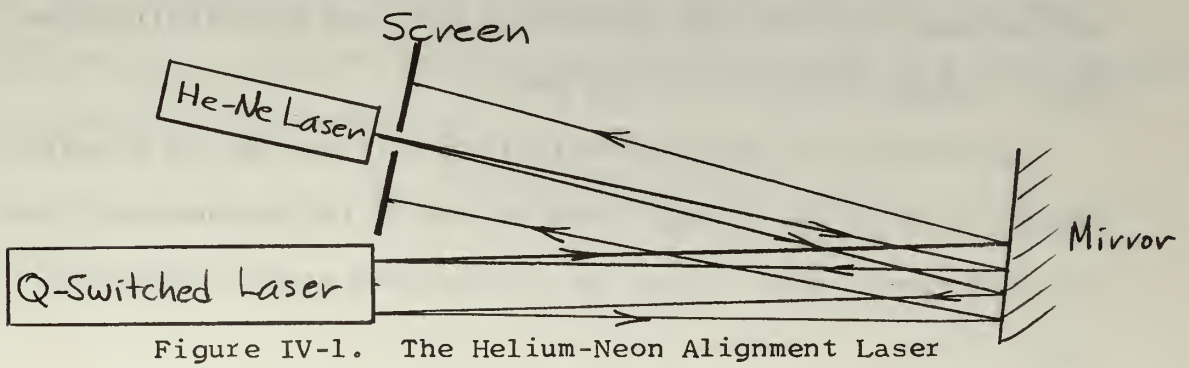

Figure IV-1. The Helium-Neon Alignment Laser

The first step in alignment was to set the critical spacings L_1 through L_6. It is estimated that a precision of about 0.2 millimeter was attained in the more critical of these spacings. Lateral and vertical shifts to assure that useful apertures coincided were then made using the gas laser beam as a reference. Resonant reflector flats CD and EF were tightened on their quartz spacer to give no fringes over the central region. The prism was oriented to center its folded reflection on the small hole in the screen (see Figure IV-1) and so that the reflection from its front surface did not pass back through the ruby. Finally, all the flats of the resonant front reflector together with the prism were aligned to give the least complex interference pattern. The extreme spectral narrowness of the He-Ne laser output made possible sharp interference fringes even with an effective étalon spacing of 210 centimeters. The dual aperture was inserted after aligning the reflectors and adjusted to assure exact folding by the prism of each of the spots into the other and to exploit the focii within the ruby.

It was generally necessary to repeat the above alignment cycle several times before all steps could be completed without disturbing one of the initial adjustments. The above steps were carried out with the beam deflecting flat and electrostrictive block removed from the optical path.

Adjustment of the beam deflecting flat and of the electrostrictive block was accomplished by use of the Helium-Neon laser beam and a card with a mark for the desired angle as shown in Figure IV-2.

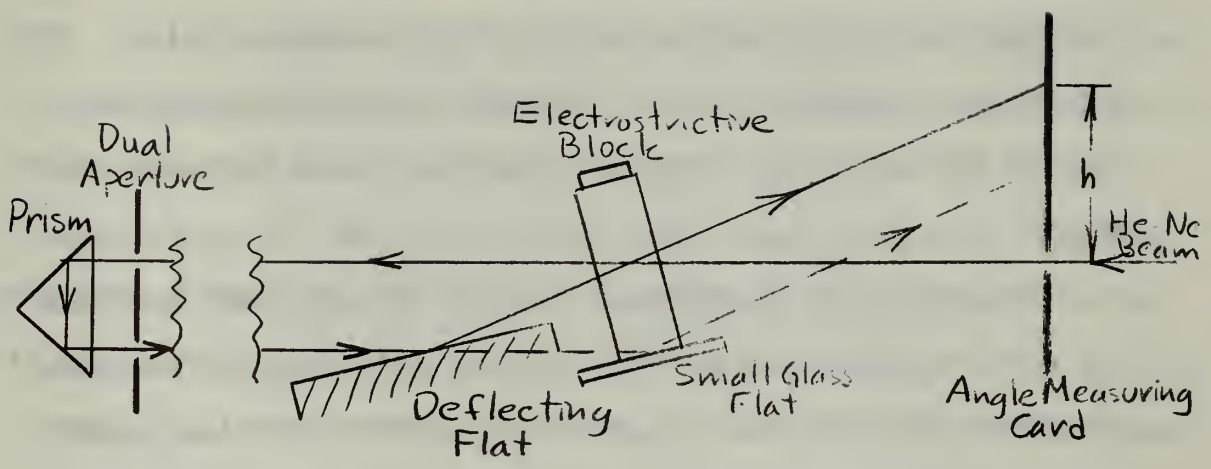

Figure IV-2. Adjusting for the Proper Intersection Angle

The angle measuring card was placed in the beam of the gas laser at a distance of 1.5 meters from the electrostrictive cell. The three millimeter hole in the card was positioned to coincide with the upper hold in the dual aperture.

Bonded to the bottom of the electrostrictive cell was a small glass flat. With the beam deflecting flat removed, the folded beam was reflected off this flat to cast a pattern with poor vertical resolution, but moderate lateral resolution on the angle measuring card. The coaxial cavity holding the electrostrictive block was adjusted in the roll angle to position the pattern reflected by the small flat on a vertical line above the hole in the card. Tilting the coaxial cavity and block adjusted the height of the spot reflected from the front of the block to a mark scribed on the card at a height of

$$h = 300 \cos^{-1} \frac{\lambda_1 f_s}{2 v_s} \text{ cm.} \qquad \text{(IV-1)}$$

This equation can be simply derived from Equation (II-12). This adjustment, together with the roll adjustment described above assured that the sound wave fronts were parallel with the transducer.

The precision of numbers available for the light wavelength, λ_l, and the acoustic frequency, fs, was very good. Precision of the number for the velocity of sound in the material, v_s, was improved to about $\pm$ 1% by using a Brillouin scattering test. The blocks were excited with continuous 250 megahertz acoustic waves and the angle thru which the helium neon beam scattered was measured. The sound velocity was then computed by inverting Equation (IV-1).

The deflecting flat was inserted and adjusted so that the reflected folded beam struck the card at the correct height, h, and on the vertical line above the hole. This assured the correct angle between the two light beams.

Tuning of the Signal Detection System

A straightforward procedure using the pulsed oscillator sufficed to tune the detection system. Probably due to thermal expansion, the tuning of the coaxial cavity was found to drift seriously during the course of a run. Thus it was necessary to check the tuning with the pulsed oscillator before every firing of the system. While firing for sound, the amplitude of the pulse generator was reduced to zero and its trigger generator disabled.

Procedure for Data Runs

After completing all aligning and tuning, an exposed polaroid print was positioned in front of the angle measuring card to check by the burned spots that the Q-switched laser beam was firing where expected. While the laser power supply capacitor bank was charging, the type 555 oscilliscope trigger was changed from the external synchronising pulse out of the pulse generator to the PIN Photodiode. The oscilloscope triggers were operated in the single sweep mode. Both oscilloscope camera shutters were operated manually in the B or bulb mode to be open when the Q-switched laser was fired.

V. EXPERIMENTAL RESULTS

Figure V-1 shows oscilloscope traces of the detected acoustic signal from the coaxial cavity and of the photo current produced in the PIN photodiode. Trace A was the photo-diode output which was recorded simultaneously and on the same time scale with the detected acoustic pulse, trace B, on all of the later experimental trials. The same trigger circuitry and sweep generation was used for both the photodiode and detector signals. Thus the time of the detector signal could be precisely compared with the time of the light pulse. The time lag of the start of the detector signal after the laser pulse found by comparing Trace B with A and B' with A' was about 0.5 microseconds. Some variation in this delay was noted with the longest delays being 0.75 microseconds and the shortest delays being 0.40 microseconds. Traces A and B were displayed on a Tektronix type 555 double beam oscilloscope and photographed on Polaroid film with an ASA speed of 3,000.

The photodiode output was also displayed on a Tektronix type 519 oscilloscope which had a frequency response up to one gigahertz. The sweep speed of 20 nanoseconds per centimeter allowed only the leading edge of the photodiode output to be displayed but it did permit the beat signal at 490 Megahertz to be easily seen. The trace was recorded using a Tektronix ultra high writing speed camera and Polaroid film with an ASA speed of 3000.

Throughout the experimental trials in which photodiode output was displayed and recorded at a high sweep speed, the resonant reflector spacings were arranged to cause multi-mode lasing with a frequency separation of 490 MHz. The beat frequency seen by

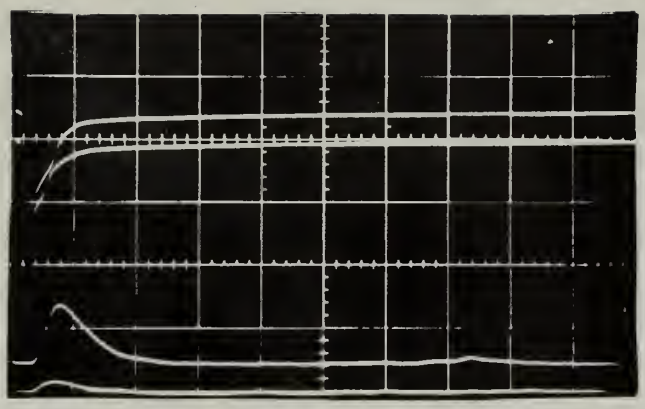

Traces A and A' are the photo diode signals when the laser was fired. Traces B and B' are the amplified I.F. envelopes derived from the tuned coaxial cavity. A and B are of one event, A' and B' of another. The horizontal scale is 2 microseconds per division.

Traces C and C' are the photodiode signals with a high sweep speed to show beating between modes. The horizontal scale is 20 nanoseconds per division.

Figure V-1. Oscilloscope Trace Photographs

the photodiode was determined by counting cycles over the portion of the sweep photograph where they were clearly distinguishable. The beats measured in this way varied from 475 MHz to 500 MHz with an estimated precision in measuring of 3 MHz. This variation in beat frequency implies an effective variation in the resonant reflector length, L_3, and in the overall laser cavity length, L_4. Such was entirely possible. The surfaces in the resonant reflector which were antireflective coated were considered in the design of the reflector to have zero reflectivity, but in reality reflected one third as much intensity as the uncoated surfaces. Thus, the extra surfaces could be expected to shift the frequency intervals in the reflectivity combs. The appearance of beats on the photodiode output was observed on 24 out of 35 trials in the two final series of data trials. It was observed that, with very few exceptions, beats were produced only when the optical pumping power was between 25 and 40 percent above the threshold for giant pulse lasing. Some of the photodiode current beats which were recorded showed a variation which was not a smooth sine wave. A few of the beat waves had a uniformly repeated non-symmetry which indicated the presence of a second harmonic of the 490 MHz beat. This would be just the effect of three instead of two longitudinal modes lasing simultaneously. The separations between each adjacent pair would be 490 MHz, while the separation between the two outer modes would be 980 MHz, or the second harmonic.

One characteristic of the pulses produced by the detection system, examples of which are traces B and B' in Figure V-1, which was not clearly comprehensible was the fact that they were

observed to start about 0.5 microseconds after the laser pulse. The time of acoustic propagation from the directly illuminated region of the glass block to the transducer should have been about 1.8 microseconds. However the peak of the pulses was at the proper time so the early forward slope could have been due to light reflected by the uncoated walls of the block to beat electrostrictively nearer the transducer.

Several other factors, however, support identifying the pulses produced by the detector as sound generated by electrostrictive beating of the two laser beams.

Perfect correlation was found between the appearance of pulses in the detector signal and a relatively strong beat in the photodiode output.

High acoustic attenuation in the flint glass, about 5 db per centimeter at 490 MHz, and errors in parallelism between the two end faces of the block were sufficient to account for the non-existence or weakness of echos. Removal of the piece of microscope slide, which had been cemented to the bottom end of the glass block to assist in aligning, improved the acoustic reflection at the bottom and resulted in the appearance of faint echos like that seen on trace B in Figure V-1. The time of occurrance of the echo and its amplitude were consistent with the known acoustic velocity and attenuation.

Removal of the deflector flat, which caused the lower laser beam to intersect with the upper in the glass block or tilting the glass block so that the acoustic wave would not impinge

perpendicularly upon the transducer resulted in no pulses appearing. Even very slight maladjustments of the critical angles, errors as small as a few minutes of arc, appeared to be sufficient to prevent the generation or detection of the acoustic pulses.

The above evidence is considered sufficient to conclude that the intersection of the two beams, each containing light at more than one frequency, produced acoustic pulses at the difference frequency by electrostrictive beating.

A careful determination of the frequency bandwidth of the acoustic waves produced was not accomplished. Before this could be done one end of the ruby laser crystal began to develop cracks which made reliable lasing impossible. However, the appearance of pulses with the detector tuned to 490 MHz and the photodiode beats varying from 475 to 500 MHz indicated a bandwidth of at least $\pm$ 15 MHz.

VI. CONCLUSIONS

The use of two longitudinal modes of the same laser is the first successful procedure, to our knowledge, which produces light at two or more precisely and predictably different frequencies without relying upon Brillouin scattering. This new procedure makes electrostrictive beating a primary source of an intense, pulsed beam of hypersound. In contrast, the procedure of Korpel and of Caddes, while providing the first demonstration of electrostrictive beating, served only to inject the sound where it was wanted, if it were first generated by a conventional transducer elsewhere. The potentials, both in peak power and in frequency, of which the procedure is capable are far in excess of the previously available, externally attached transducer. (Electrostriction can be thought of as a means of making the acoustic medium serve as its own transducer, the energy conversion being from light to acoustical rather than from electrical to acoustical.) This first trial has been conducted in a frequency band where piezoelectric transducers are also practicable and indeed quite efficient. This has permitted monitering the sound generated with a conventional transducer. The exclusive domain of electrostrictive beating is much higher in frequency, from a few gigahertz, where piezoelectric transducers become too thin to convert useful power levels, up to about 50 gigahertz, an average of the upper limit for the phenomenon.

Both the doppler shifting technique and the use of an intercavity Brillouin cell, alternatives listed in the introduction, appeared in preview to be more workable procedures for generating

the two light beams of different frequencies. Hence these two approaches were attempted first. Early attempts to force the giant pulse laser to lase in a single, spectrally narrow mode were only marginally successful. Hence, attempting to force lasing in two spectrally narrow modes with a precise and predictable frequency difference was at first considered futile. The use of a pair of longitudinal modes was found, however, to accomplish the purpose with none of the complex moving parts of the doppler machine which were difficult to build and operate. The auxiliary acoustic system required in the intercavity scattering approach is also eliminated. The extreme difficulty encountered in the two first approaches made the simplicity of construction, and ease of nominal success with the pair of longitudinal modes, appear quite striking.

At the time of the writing of this report, this new method for generation of an intense, pulsed beam of hypersound has not been refined to the state of being a readily usable laboratory tool. The new techniques for forcing the desired dual mode lasing have been developed and demonstrated and their applicability to electrostrictive beating shown. However, further development is required before the method can be used as a reliable and predictable source of hypersound for other investigations.

The complex and asymmetrical reflection pattern produced by the optical components, even when very carefully adjusted to give the least complex and most symmetrical interference pattern

possible, indicate that the prime need for improvement is in the precision of the optical components.

The ruby laser crystal should be replaced by one that does in fact meet or exceed the specifications given in Section III. The apparent very short life of the end surfaces of the crystal, when used to produce a pair of longitudinal modes, indicates that interference may be occuring which causes intense phonon production near the surface of the ruby. Perhaps this could be alleviated by using a square ended ruby crystal with multi-layer dielectric anti-reflection coating on the ends.

The total internal reflection prism used for the rear end reflector has been observed to deteriorate rapidly. Perhaps the most economical soution to this problem is frequent lateral shifting of the prism to utilize different portions of the roof edge and periodic replacement.

The sapphire flats used in the resonant reflector, with a flatness of better than one tenth wavelength and a wedge less than two seconds of arc would probably be sufficient, but the dense glass flats which were also used definitely were not good enough. Instead of the locally applied single coating of magnesium fluoride, the anti-reflective coating should be mutli-layer and peaked for minimum reflectance at the ruby emission wavelength.

The large flat used for external bending of the lower of the two beams from the laser should be flat within one tenth wavelength and thick enough to maintain this flatness over its entire length.

The flint glass in which the electrostrictive beating was done appears to be a good material, however the parallelism of the six by ten millimeter end faces needs to be improved. The original specification, parallelism within ten seconds of arc, would be adequate. The block used had a parallelism error of two minutes of arc.

The expense of the cadmium sulfide piezoelectric transducer used to monitor the sound is considered, in retrospect, to be unnecessary. Quartz transducers operated at moderate overtones appear to be as efficient. The predictability of the frequency produced by the new procefure together with the apparent broad bandwidth of the phenomenon makes the continuous sensitivity of the CdS transducer unnecessary.

The above noted improvements in the optical components are expected to improve the repeatability of the system sufficiently that several quantitative measurements can be taken that may be of value in applying the new method to other investigations. First, the validity of the arguments used in locating the components within the laser can be checked. Second, the bandwidth of the acoustic pulses produced can be determined. Third, the tolerances which must be maintained in adjusting the angles of the intersection can be found. Fourth, the efficiency of the interaction could be measured to see if it actually approaches the limit of

$$P_S = \frac{f_S}{f_L} P_L \qquad \text{(VI-1)}$$

where

P_s is acoustic power

P_L is light power in one beam at one frequency

f_s is acoustic frequency

f_L is light frequency

The above improvements and measurements appear, in preview, to be what must be done to refine the method from the present demonstrated workable procedure to a predictable tool which can be included, with only tolerable uncertainty, in the design of experiments requiring intense pulsed hypersound beams.

BIBLIOGRAPHY

1. Brillouin, L., "Diffusion de la Lumière et des rayons x par un corps transparent homogene", Ann. Phys. (Paris), 9th Ser., Vol. 17, p.88, 1922.

2. Brillouin, L., La Diffraction de la Lumière par des Ultra-Sons, Hermann (Paris), 1933.

3. Debye, P., and Sears, F.W., "On the scattering of light by supersonic waves", Proc. Nat'l Acad. Sci. (USA), Vol. 18, p. 409, 1932. Lucas, R., Biquard, P., Optical properties of solids and liquids under ultrasonic vibrations", J. Phys. Rad., 7th Ser., Vol. 3, p. 464, 1932.

4. Ali, L., "Uber der Nochweis der Frequen zanderung des Lichtes durch der Doppler effekt bei der Licht bengung an Ultra schallwellen in Flussigkeiten", Helv. Phys. Acta, Vol. 8, p. 503, 1935; Vol. 9, p. 63, 1936.

5. Cummins, H.Z., and Knable, N., "Single sideband modulation of coherent light by Bragg reflection from acoustical waves", Proc. IEEE, Vol. 51, p. 1246, Sept 1963.

6. Korpel, A., Adler, R., and Alpiher, B., Direct observation of optically induced generation and amplification of sound", Appl. Phys. Ltrs., Vol. 5, p. 86, 1964.

7. Caddes, D.E., Quate, C.F., and Wilkinson, C.D.S., "Conversion of light to sound by electrostrictive mixing in solids", Appl. Phys. Ltrs., Vol. 8, p. 309, 1966.

8. Siegman, A.E., Quate, C.F., Bjorkholm, J., and Francois, G., "Frequency translation of a laser's output by acoustic output coupling", Appl. Phys. Ltrs., Vol. 5, p.1, 1964.

9. Buhrer, C.F., Fowler, V.J., Bloom, L.R., "Single-sideband suppressed-carrier modulation of coherent light beams", Proc. IRE, Vol. 50, pt. 3, p. 1827, 1962.

10. Kaminon, I.P., "Microwave modulation of the electro-optic effect in KH_2PO_4", Phys. Rev. Ltrs., Vol. 6, p. 528, May 1961.

11. Hercher, M., "Single mode operation of a Q-switched ruby laser", Appl. Phys. Ltrs., Vol. 7, No. 2, p. 39, 1965.

12. Rosser, W.G.V., An Introduction to the Theory of Relativity, Butterworth (London), 1964.

APPENDIX A.

Analysis of Resonant Reflectors by Signal Flow Graphs

1. The traditional treatment, as carried out by Houstoun[1] to analytically express the total reflectivity of both faces of a parallel faced glass flat, leads to

$$R^2 = \frac{4r^2 \sin^2 \frac{2\pi L}{\lambda}}{1 - 2r^2 \cos \frac{4\pi L}{\lambda} + r^4} \qquad \text{(A-1)}$$

where R is the total amplitude reflectivity

r is the reflectivity of one surface

L is the thickness of the flat

λ is the wavelength inside the flat.

Equation A-1 has maxima of

$$R^2 = \frac{4r^2}{(1+r^2)^2} \qquad \text{(A-2)}$$

at

$$L = \frac{2m+1}{4}\lambda \qquad \text{(A-3)}$$

or as a function of λ at intervals of

$$\Delta\lambda = \frac{\lambda^2}{2L} \qquad \text{(A-4)}$$

The variation of intensity of reflection with wavelength for a fixed flat thickness is shown in Figure A-1a.

2. Extension of the traditional procedure used to develop Equation (A-1) becomes intractable when dealing with three or more surfaces. An approximate picture of total reflectivity for three or more surfaces can be produced as shown in Figure A-1b by a graphical superposition of two combs of reflectivity, one with peaks at intervals of $\lambda^2/2L_1$, the other with peaks at

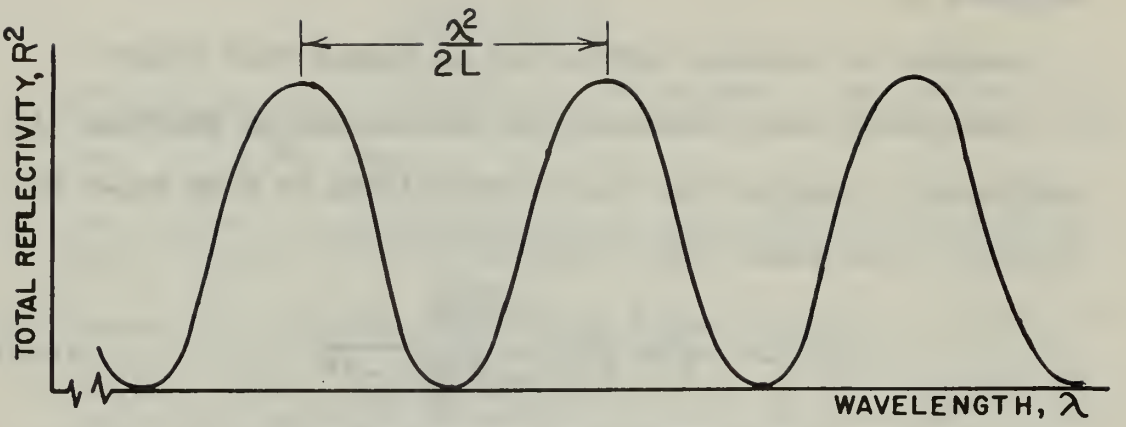

a. TWO SURFACES WITH OPTICAL SPACING L

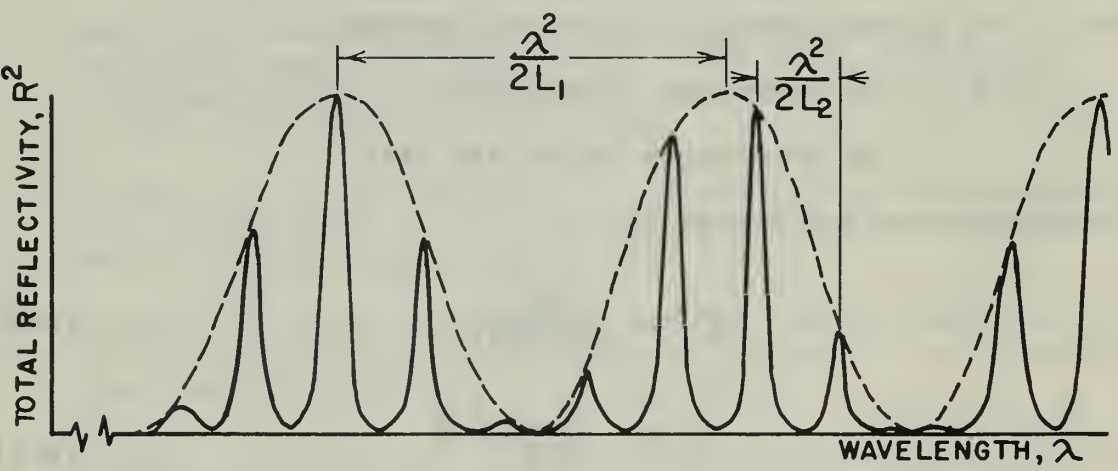

b. THREE SURFACES WITH OPTICAL SPACINGS IN THE RATIO $L_2 : L_1 = 5.2 : 1$

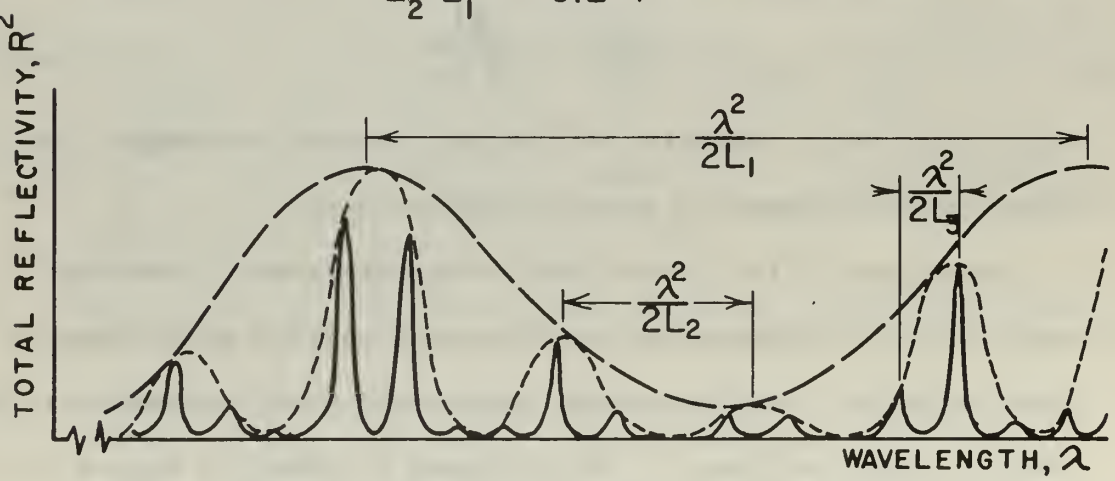

C. FOUR SURFACES WITH OPTICAL SPACINGS IN THE RATIO $L_3 : L_2 : L_1 = 13 : 3.5 : 1$

FIGURE A-1

COMBS OF REFLECTIVITY OF PLANE, PARALLEL, PARTIALLY REFLECTIVE, MULTIPLE SURFACE, RESONANT REFLECTORS

intervals of $\lambda^2/2L_2$. This graphical method does not, however, provide a quantitative measure of the shifts in the fine comb spacing, which become significant if L_2 is not much greater than L_1, nor does it yield an exact value of the reflectivity at the peaks.

3. Analysis by signal flow graph[2] technique is suggested by the linear nature of the resonant reflector system and by the importance of multiple reflections in determining the detailed behavior, much as feed back loops dominate the behavior of many linear lumped bilateral networks. The following treatment is not intended to introduce the use of signal flow graphs, but only to show their application to the problem at hand.

An assignment of variables which lends itself to Mason's signal flow graph analysis of the system is shown in Figures A-2a, b, and c for a single flat reflector, a three surface reflector, and a four surface reflector. The variable, A^+ represents the amplitude and phase of light incident upon the first surface from the left, B^+ the amplitude and phase of light incident upon the second surface from the left, etc., B^-, for example, is not simply the first reflection returned to impinge upon the left surface, but is the vector infinite sum of all multiple reflections which inpinge upon the left surface from the right. A^- is seen to be the total reflected light amplitude which is of most interest in analysis of a resonant reflector. The surface spacings, L_i, are effective optical lengths, having been corrected by the index of refraction in the region.

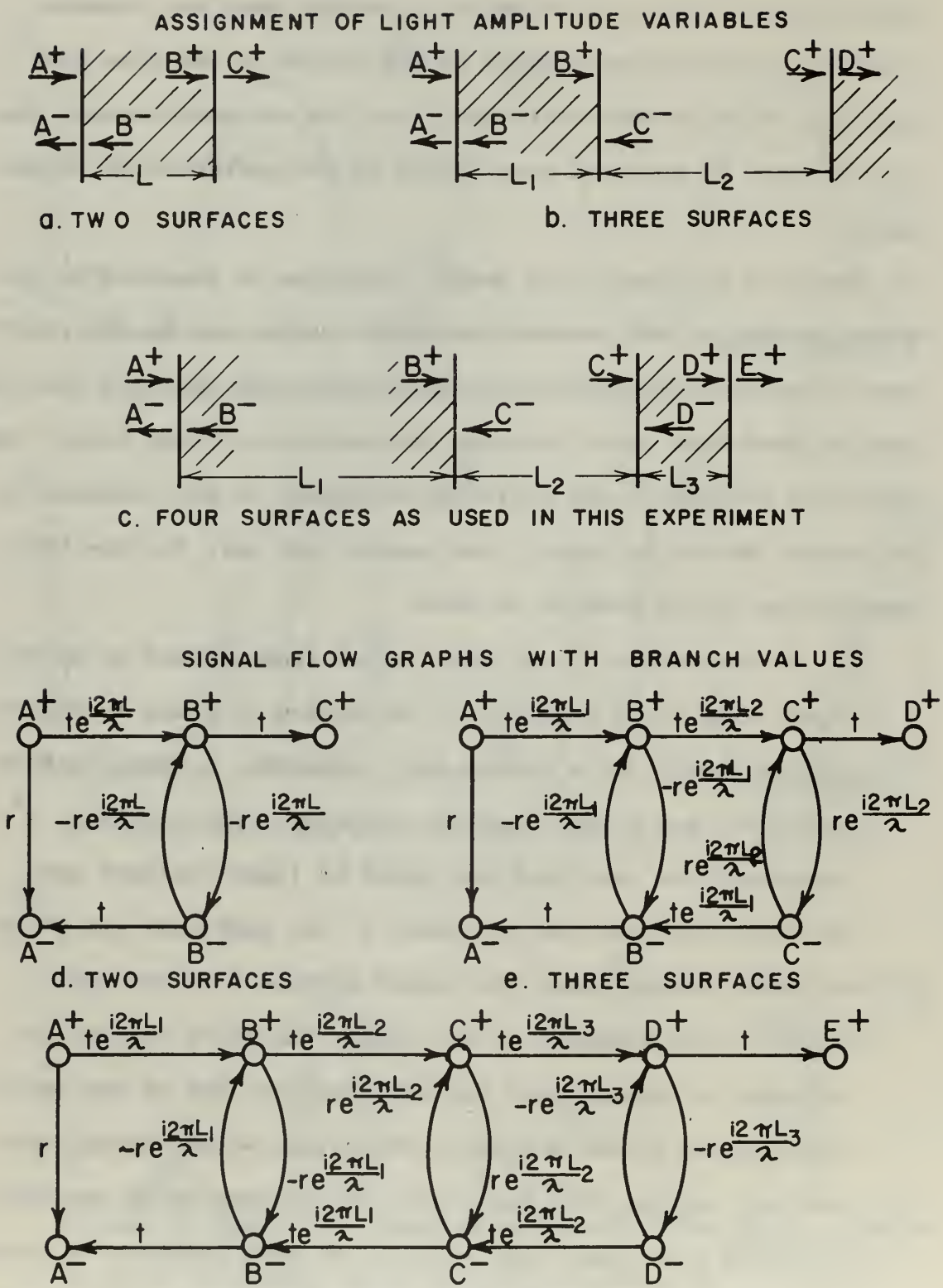

FIGURE A-2

ASSIGNMENT OF VARIABLES AND FLOW GRAPHS FOR ANALYSIS OF RESONANT REFLECTORS

The signal flow graphs with the values of the branch operators, Figures A-2d, e and f can be drawn by inspection using Mason's concepts. The coefficient of amplitude reflection, r, need not be the same at every surface. The light wavelength is as measured in free space. The transmission coefficient, t, for a loss-less interface can be replaced by $1-r^2$, or can be different if the surface has non-zero absorption.

Application of Mason's generalized gain formula allows one to write directly from Figure A-2a,

$$\frac{A^-}{A^+} = \frac{-rt^2 e^{\frac{i4\pi L}{\lambda}} + r\left(1-r^2 e^{\frac{i4\pi L}{\lambda}}\right)}{1-r^2 e^{\frac{i4\pi L}{\lambda}}} \qquad \text{(A-5)}$$

which simplifies to

$$\frac{A^-}{A^+} = \frac{r\left(1-e^{\frac{i4\pi L}{\lambda}}\right)}{1-r^2 e^{\frac{i4\pi L}{\lambda}}} \qquad \text{(A-6)}$$

This can be shown to be equivalent to Equation (A-1), so has the same maxima and intervals between maxima.

Similarly, Mason's generalized gain formula applied to the 3 surface problem yields directly from Figure A-2d,

$$\frac{A^-}{A^+} = r\,\frac{-rt^2 e^{\frac{i4\pi L_1}{\lambda}}\left(1-r^2 e^{\frac{i4\pi L_2}{\lambda}}\right) + rt^4 e^{\frac{i4\pi(L_1+L_2)}{\lambda}}}{1-r^2 e^{\frac{i4\pi L_1}{\lambda}} - r^2 e^{\frac{i4\pi L_2}{\lambda}} + r^2 t^2 e^{\frac{i4\pi(L_1+L_2)}{\lambda}} + r^4 e^{\frac{i4\pi}{\lambda}(L_1+L_2)}} \qquad \text{(A-7)}$$

Equation A-7 can be simplified and the maxima found to occur if there exists a wavelength at which

$$L_1 = (p + \tfrac{1}{4})\lambda \tag{A-8a}$$

and

$$L_2 = (q + \tfrac{1}{4})\lambda \tag{A-8b}$$

where p and q are integers

The value of these best possible maxima then is

$$\frac{A^-}{A^+} = \frac{3r}{1+2r^2} \tag{A-9}$$

Application of Mason's gain formula to the flow graph of Figure A-2f yields the reflectivity function for the four surface reflector used in this experiment. The algebra becomes ponderous, but entirely workable. Again the highest maxima can be expected to occur when

$$L_1 = (p + 1/4)\lambda \tag{A-10a}$$

$$L_2 = (q + 1/4)\lambda \tag{A-10b}$$

$$L_3 = (s + 1/4)\lambda \tag{A-10c}$$

where p, q, and s are integers, if such a wavelength exists. These best possible maxima have a value

$$\frac{A^-}{A^+} = \frac{4r(1+r^2)}{1+6r^2+r^4} \tag{A-11}$$

Though the procedure for writing Equation (A-7) is straightforward, and indeed has been extended to study a reflector with four surfaces, it is already, with three surfaces becoming difficult to extract detailed information about the behavior of the system.

4. The analog computer is suggested as a convenient and powerful tool for future study of the behavior of resonant reflectors, but most importantly as an aid in their design. It has been shown that drawing the signal flow graph of a resonant reflector is easily carried out. The analog computer circuitry could be developed on the basis of the signal flow graph. The reflectivity versus wavelength curves like Figure A-1b could then be plotted on an X-Y recorder and the effect of changes in reflectivity of any surface, in spacings and in number of surfaces determined in order to design reflectors of the desired characteristics.

1. Houston, A Treatise on Light, Longmans, Green (London), 1930.

2. Mason, S.J., "Feedback theory, some properties of signal flow graphs", Proc. IRE, Vol. 41, p. 1144, Sept. 1953, and Vol. 44, p. 920, July 1956.

APPENDIX B.

The Doppler Shifting Approach

Of the four alternative methods enumerated in the introduction for obtaining two laser beams at slightly different frequencies for electrostrictive beating, the first one attempted in the course of this experiment was Doppler shifting. Figure B-1 shows in schematic form the apparatus which was developed.

The laser cavity was made very long, up to 1.5 meters, to reduce divergence, stretch the pulse duration and hopefully to improve coherence. Several different configurations of the laser components were tried with both ruby and neodymium doped glass rods. The laser output beam, after being coupled out of the cavity and split, was reflected by mirrors on the ends of a spinning rotor which imparted to one beam a positive Doppler shift and to the other beam a negative Doppler shift. By causing each beam to be reflected twice consecutively by the 33.5 centimeter long rotor, a speed of 2400 revolutions per minute gave a beat frequency of 500 megahertz between the two ruby laser light beams. A mirror system was devised using a 90^{o} roof mirror on the rotor and a fixed plane mirror which eliminated angular and linear sweep of the reflected beam in the duration of the light pulse.

Assurance that the laser would fire only as the rotor passed through position was given by mounting the roof prism rear reflector of the laser on the rotor shaft. Optical pumping of the laser rod was commenced at the proper interval of time before the prism and rotor came into alignment by a special trigger and

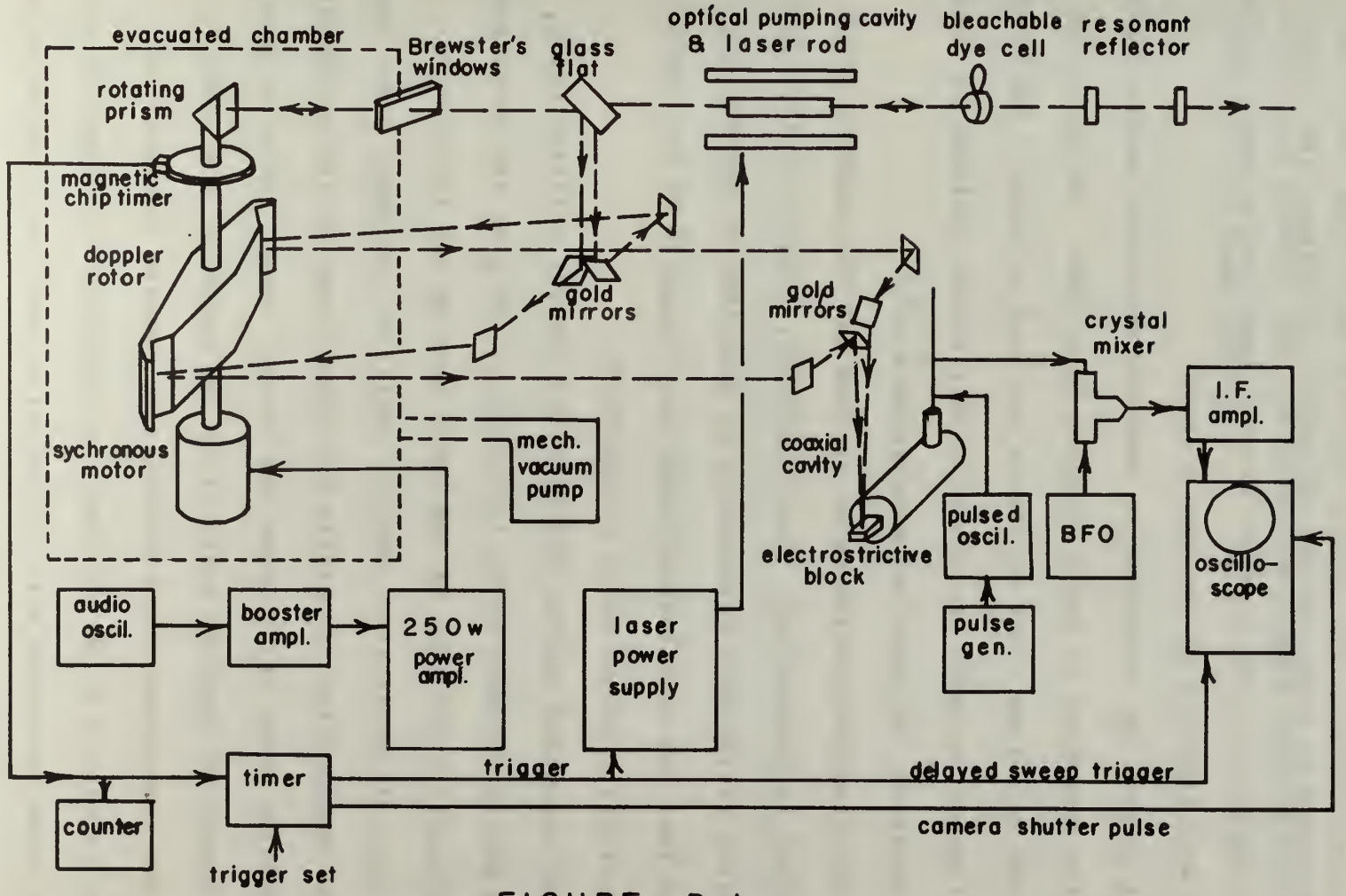

FIGURE B-1

SCHEMATIC OF PHONON GENERATION BY DOPPLER SHIFTING AND ELECTROSTRICTIVE BEATING OF A LASER BEAM

timing circuit designed and built for the apparatus. A magnetic chip rotating with the rotor induced a pulse in a pick-up coil which turned on a silicon control switch to trigger the laser power supply. An oscilloscope trace trigger and a camera shutter pulse were provided by the same circuit.

A process was developed to make mirrors which would withstand repeated exposures to the Q-switched laser beam. An optically polished stainless steel substrate was used on which a few hundred Angstroms of chromium was evaporatively coated followed by about 3000 Angstroms of spectroscopically pure gold.

The electrostrictive material used was the sapphire block described in Section III. The transducer, coaxial cavity, and detection system were essentially as described in Section III, except that the oscilloscope sweep was triggered by the special timer circuit instead of by a photodiode.

An evacuated chamber enclosed the Doppler shifting rotor, prism and synchronous motor to reduce air drag on the rotor and to eliminate refraction of the laser beam by air turbulence.

An audio oscillator, booster amplifier and large power amplifier provided the adjustable frequency power to the hysteresis synchronous motor which drove the rotor. Actual rotation speed was checked by counting pulses from the magnetic chip timer.

The system was quite difficult to operate and required several hours to align and tune. A few hundred attempts to observe sound were made with various minor modifications before one of the mirrors broke loose from the rotor and damaged all optics

inside the evacuated chamber. It was presumed, though not verified before the rotor failed, that the principal difficulty was due to the optical path from the laser to the electrostrictive material being much greater than the coherence length (not directly measured) of the laser output.

INITIAL DISTRIBUTION LIST

		No. Copies
1.	Defense Documentation Center Cameron Station Alexandria, Virginia 22314	20
2.	Library Naval Postgraduate School Monterey, California 93940	2
3.	Naval Ship Systems Command Code 2052 Navy Department Washington, D.C. 20360	1
4.	Electronics Systems Command Headquarters Bailey's Crossroads, Virginia 22041	1
5.	Prof. E. C. Crittenden, Jr. Department of Physics Naval Postgraduate School Monterey, California 93940	5
6.	Prof. Warren B. Boast, Head Department of Electrical Engineering Iowa State University Ames, Iowa 50010	1
7.	LT N. Leon Wardle 1108 Murray Drive Ames, Iowa 50010	3

UNCLASSIFIED
Security Classification

DOCUMENT CONTROL DATA - R & D

(Security classification of title, body of abstract and indexing annotation must be entered when the overall report is classified)

1. ORIGINATING ACTIVITY *(Corporate author)*
Naval Postgraduate School
Monterey, California 93940

2a. REPORT SECURITY CLASSIFICATION
UNCLASSIFIED

2b. GROUP

3. REPORT TITLE
Hypersound from Electrostrictive Beating of Longitudinal Laser Modes

4. DESCRIPTIVE NOTES *(Type of report and inclusive dates)*
Thesis, Ph.D., June 1968

5. AUTHOR(S) *(First name, middle initial, last name)*
Norval Leon Wardle, LT, USN

6. REPORT DATE	7a. TOTAL NO. OF PAGES	7b. NO. OF REFS
June 1968	64	12

8a. CONTRACT OR GRANT NO.	9a. ORIGINATOR'S REPORT NUMBER(S)
N/A	N/A
b. PROJECT NO.	
c.	9b. OTHER REPORT NO(S) *(Any other numbers that may be assigned this report)*
d.	N/A

10. DISTRIBUTION STATEMENT
[redacted] to foreign nations may be made only with prior approval of the Naval [redacted]

11. SUPPLEMENTARY NOTES

12. SPONSORING MILITARY ACTIVITY
Naval Postgraduate School

13. ABSTRACT

A new method for generating pulses of hypersound by electrostrictive beating of two coherent light beams has been demonstrated. Three new procedures for generating the two required beams with a precise and predictable difference between their frequencies have been experimentally investigated. In the most practical of these a giant pulse ruby laser was forced to emit light at two frequencies. Techniques to control the difference between the two frequencies have been developed which depend solely upon the locations of the standard laser components and the spacings between the several glass flats which serve as one end mirror. The two laser beams have been intersected in flint glass to beat electrostrictively and produce intense, pulsed acoustic beams at 500 megahertz. The value of the method lies in its potential of producing much higher intensities and frequencies than do the conventional piezoelectric transducers.

DD FORM 1 NOV 65 1473 (PAGE 1)
S/N 0101-807-6811

UNCLASSIFIED
Security Classification

A-31408

14. KEY WORDS	LINK A		LINK B		LINK C	
	ROLE	WT	ROLE	WT	ROLE	WT
Electrostriction						
Electrostrictive Beating						
Hypersound						
Acoustic Wave Generation						
Laser Mode Control						
Q-switched Laser						
Light-Sound Interaction						
Resonant Reflector						
Longitudinal Modes